Science of the Total Environment 660 (2019) 1327–1337

Contents lists available at ScienceDirect

Science of the Total Environment

journal homepage: www.elsevier.com/locate/scitotenv

Evidence of the mitigated urban particulate matter island (UPI) effect in China during 2000–2015

Xin Huang [a,b], Yafang Cai [a], Jiayi Li [a,*]

[a] School of Remote Sensing and Information Engineering, Wuhan University, Wuhan 430079, People's Republic of China
[b] State Key Laboratory of Information Engineering in Surveying, Mapping and Remote Sensing, Wuhan University, Wuhan 430079, People's Republic of China

HIGHLIGHTS

- The concept of urban particulate matter island (UPI) is defined.
- The UPI phenomenon is verified in China based on the observations in 338 prefectures.
- UPI intensity (UPII) and UPI footprint (UPIFP) varied by cities and climatic zones.
- The land use/cover change is essential for the mitigation of UPI during 2000–2015.
- Cities with faster expansion and more residents show steeper decline of UPII in China during 2000–2015.

GRAPHICAL ABSTRACT

$PM_{2.5}$ concentration trends and corresponding built-up and vegetation proportions from urban to background areas.

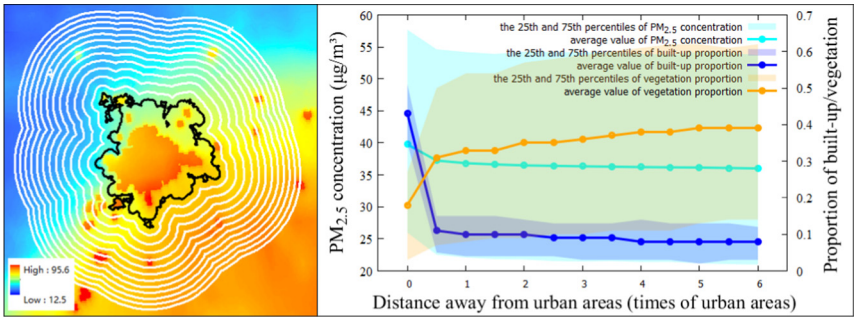

ARTICLE INFO

Article history:
Received 13 November 2018
Received in revised form 25 December 2018
Accepted 9 January 2019
Available online 11 January 2019

Editor: Pavlos Kassomenos

Keywords:
Urbanization
Urban particulate matter island (UPI)
Spatiotemporal patterns
China

ABSTRACT

Urban fine particulate matter ($PM_{2.5}$) pollution has been the subject of great concern, due to its remarkable adverse effects on public health. However, quantitative investigations of the spatial concentration trends from urban to background areas are still lacking. The urban particulate matter island (UPI) effect, referring to the phenomenon that higher particle concentrations in urban areas are gradually attenuated to background areas, is found and investigated in this study. UPI intensity (UPII) and its footprint (UPIFP) are defined to quantify the magnitude and extent of UPI, respectively. Based on observations from 338 Chinese prefectures for 2000–2015, we confirm the existence of the UPI effect, and further reveal its spatiotemporal patterns. We find that: 1) 84% (283/338) of the cities in China in various city levels and climatic zones showed the UPI phenomenon during 2000–2015, and this phenomenon is closely related to the land-use/cover patterns between the urban area and surrounding areas; 2) different spatial patterns of UPI effect are apparent, with high UPII values and small UPIFP values in Beijing-Tianjin-Hebei, moderate UPII values and large UPIFP values in northern China, the Pearl River Delta and the Yangtze River Delta, and high UPII and UPIFP values in the Western Taiwan Straits region; 3) UPI mitigation can be observed nationwide, with significant decreasing trends for both UPII and UPIFP, benefiting from the increase in urban green spaces and the built-up proportion differences between urban and suburban areas during urbanization. Additionally, it is indicated that more urban residents and faster urban expansion correspond to a steeper decline of UPII in China during 2000–2015. The existence and characteristics of the UPI effect in China will allow new insight and understanding of urban pollution patterns, and will provide scientific evidence for urban planning and pollution control.

* Corresponding author.
E-mail address: zjjerica@whu.edu.cn (J. Li).

https://doi.org/10.1016/j.scitotenv.2019.01.099
0048-9697/

1. Introduction

Anthropogenic activities are transforming the agriculture-dominated rural society to an industry-dominated urban society at an unprecedented rate worldwide (Wu, 2008; Seto et al., 2011), which is also known as "urbanization". By 2010, more than half of the global population lived in urban areas, and the proportion is projected to reach 66.4% by 2050 (*WUP*, 2014). Accelerating urbanization has profoundly modified the Earth's systems (Wu et al., 2011) and damaged the ecological environment (Cumming et al., 2014), triggering severe environmental problems such as air pollution (Larkin et al., 2016), urban heat islands (Zhou et al., 2014a), global climate change (Grimm et al., 2008), water pollution (Noorhosseini et al., 2017), and infectious diseases (Zhu et al., 2011). Moreover, as long as the urban population continues to grow, the rapid pace of urbanization will not stop (Angel et al., 2011), signifying huge potential threats to human health. As one of the most alarming problems, fine particulate matter ($PM_{2.5}$) pollution in many urban areas has been the subject of great concern, due to its remarkable adverse effects on public health (Pope et al., 2011; J. Liu et al., 2016). It has been shown that air pollution, mostly $PM_{2.5}$, leads to 3.3 million premature deaths annually worldwide (Lelieveld et al., 2015). Therefore, to provide evidence for urban pollution control, a better understanding of the characteristics of urban $PM_{2.5}$ pollution is of great importance.

Owing to the diversity of human activities and the local climate conditions (Rubel and Kottek, 2010), urban areas and their surrounding areas can exhibit significantly heterogeneous distributions of $PM_{2.5}$ concentration in different cities. From the perspective of anthropogenic activities, on the one hand, the massive manmade emissions in urban areas can aggravate the pollution and result in higher concentrations than their surrounding areas (Bressi et al., 2013). On the other hand, however, human efforts in urban pollution control, benefiting from ecological urban construction, can reduce $PM_{2.5}$ concentrations in urban areas, which may even display lower concentrations than their surrounding areas, especially in the regions with a harsh environment (Rowe, 2011). In terms of climate conditions, natural climatic factors can further complicate the pollution distribution. For instance, the sea–land breeze can have a remarkable impact on $PM_{2.5}$ distribution in coastal areas (Ding et al., 2004), while human activities during rapid urbanization can have noticeable effects on regional climate and disrupt the pollution transfer (Karl and Trenberth, 2003; Zhou et al., 2004). Therefore, whether and how urban $PM_{2.5}$ concentrations are higher than their surrounding areas still needs to be revealed. In this context, the specific $PM_{2.5}$ concentration patterns between urban areas and their surrounding areas require quantitative investigation, to allow us to produce guidelines for further urban planning and environmental protection.

Previous research compared $PM_{2.5}$ concentrations in urban and rural areas in a single city or several cities, based on the ground monitoring sites (Querol et al., 2004; Aldabe et al., 2011; Xu et al., 2017). However, the inconsistency in ground observations (i.e., caused by relocations of sites or instrumental updates) and disturbed environment around the sites (e.g., construction areas or roads) may lead to great uncertainties (Yin and Harrison, 2008). In recent years, the application of remote sensing techniques has evolved greatly in air quality studies (Hoff and Christopher, 2009). Utilizing the satellite derived data, the $PM_{2.5}$ concentration differences between urban and non-urban areas were quantified (Han et al., 2014). Nevertheless, the quantitative measure about the extent of surrounding areas affected by urban pollution is still lacking. Investigation of the transport pathways of air pollutants, such as back-trajectory analysis (Kong et al., 2010; Orza et al., 2012; Salvador et al., 2008), is an effective way to understand the areas influenced by pollution sources. For example, by detecting the long-range transport of air pollutants and identifying dominant flow patterns, back-trajectory analysis can help determine potential source regions of aerosol tracers and assess the areas affected by pollution transportation (Kabashnikov et al., 2014; Li et al., 2016; Yao et al., 2016). However, back-trajectory analysis is usually applied to regional-scale monitoring and extreme PM events (Hua et al., 2015; J. Zhou et al., 2016), and there are great uncertainties in the trajectory calculations resulting from numerical truncation, inaccurate wind field data or ambiguous specification of the starting positions (Stohl, 1998; Stohl et al., 2001). Moreover, the specific concentration trends from urban areas to their surrounding areas have not been portrayed. To our knowledge, Crutzen (2004), which hypothesized the spatial decay of urban pollution and attributed it to human energy production, might be the one of few studies to mention the pollution trends. However, there is no quantitative measurement of the pollution patterns from urban to surrounding areas.

In this paper, considering that cities are the major container of both air pollutants and heat energy (Grimm et al., 2008), we aim to investigate whether air pollution presents similar characteristics to heat in urban areas (i.e., the urban heat island effect), and introduce a new concept, namely, the urban particulate matter island (UPI) effect. This effect is clearly defined for the first time, referring to the phenomenon that higher particle concentrations in urban areas are gradually attenuated to background areas. Two metrics—the UPI intensity (UPII) and its footprint (UPIFP)—are designed to quantitatively delineate the UPI phenomenon. UPII quantifies the particle concentration difference between urban and background regions, and UPIFP describes the affected areas. By the use of these two metrics, both the magnitude and extent of the UPI effect can be measured.

In the existing literature, numerous studies have documented that $PM_{2.5}$ concentrations vary substantially across space and time (Van Donkelaar et al., 2010; Boys et al., 2014; Y.G. Wang et al., 2014; Peng et al., 2016; Hsu et al., 2017), which suggests that the UPI effect might also have great spatiotemporal variations. Satellite remote sensing should be a suitable approach for characterizing the spatiotemporal patterns of the UPI effect, supporting a relatively long-term investigation (i.e., since 2000) (Boys et al., 2014; Ma et al., 2014). Meanwhile, it is also capable of providing fine spatial resolution images to distinguish urban centers from their surrounding areas (Van Donkelaar et al., 2015, 2016). Thus, a comprehensive study of the spatiotemporal patterns of the UPI effect, including UPII and UPIFP, can be investigated in this study, on the basis of remote sensing data.

Compared with other countries in the world, China has experienced the most rapid urbanization over the past three decades (United Nations, 2014), and has also experienced high $PM_{2.5}$ concentrations in many cities (Van Donkelaar et al., 2010). It has been shown that 76% of the total Chinese urban residents (501 million) were affected by the $PM_{2.5}$ hazard in 2010 (He et al., 2016), and it is a problem of growing importance since the proportion of the urban population in China is projected to increase to 73% by 2050 (United Nations, 2012). Meanwhile, as the development status and climatic conditions are diverse across Chinese cities, the impact of urbanization on the UPI effect in China is heterogeneous. Consequently, China is an ideal area to explore the existence of the UPI effect, as well as its spatiotemporal patterns.

There are three main research questions addressed in this paper:

1) Does the UPI phenomenon exist in China?
2) If yes, at what magnitude and extent?
3) How has the UPI effect changed over the last decade?

Based on the observations from 338 Chinese prefectures for 2000–2015, we explored the existence of the UPI effect in each city with an exponential decay model (Bellander et al., 2001). The spatiotemporal patterns of UPII and UPIFP were further established to examine the magnitude and extent of the UPI effect, respectively. In addition, given the heterogeneous nature of the UPI effect in China, the prefecture-level cities were divided into several groups (i.e., five city levels and five climatic zones), according to their population sizes and climatic conditions. The results of this study will help to deepen our understanding of urban pollution patterns, and will guide urban planning and pollution control.

2. Study area

China, which has experienced rapid urbanization, and also severe urban $PM_{2.5}$ pollution in recent years (Van Donkelaar et al., 2010; United Nations, 2014), was selected as the study area in this research. Considering the diverse urbanization development levels and the complicated climatic conditions between cities, the 338 prefecture-level cities in China were employed to characterize the regional variation of the UPI effect, as well as its spatiotemporal dynamics.

Based on the Köppen-Geiger climate classification system (Rubel and Kottek, 2010), the study area was divided into five climatic zones (Fig. 1). These five climatic zones are characterized by diverse climatic conditions (e.g., temperature and precipitation): the equatorial and warm (EW) zone has a warm and fully humid temperate climate or equatorial monsoonal climate; the warm (W) zone features a warm temperate climate with dry winter and warm summer; the arid (A) zone has a cold and arid climate; the snow (S) zone is a snow climate type with dry winter; and the tundra and snow (TS) zone, at the Qinghai–Tibet Plateau, belongs to the tundra and snow climate, with cold winter and cool summer. In this study, the urban population size in 2010 (available at: http://www.stats.gov.cn/tjsj/pcsj/) was used to categorize all the prefectures into five levels: ≥10 million (super city, Level 1), 3–10 million (mega city, Level 2), 1–3 million (large city, Level 3), 0.5–1 million (medium city, Level 4), and <0.5 million (small city, Level 5) (F. Niu et al., 2013).

3. Methods and materials

3.1. Extraction of urban and background areas

The method proposed by Zhou et al. (2015) was adopted for delineation of the urban areas in our study, based on the land-cover map (China's Land Use/Cover Datasets (CLUDs) covering built-up and water classes) (see Supplementary materials Text S1 for details), prefectural boundaries (Hijmans et al., 2010), and elevation data (Van Zyl, 2001). Specifically, for each city, 12 buffer zones emanating outward from the urban area were gradually generated, with each covering half the size of the urban area (Fig. 2). The areas of the buffer zones that overlap with other buffers were removed in our experiments. In each buffer zone, pixels that were labeled as water bodies or those with elevations exceeding the highest point in the urban area by 50 m were excluded, as they might overshadow the urbanization effect on $PM_{2.5}$ pollution (Wang et al., 2008). The natural background was defined as the three farthest buffer zones, as suggested in Zhou et al. (2015). To monitor the temporal dynamics, urban and buffer areas from each CLUD annual map (i.e., every five years: 2000, 2005, 2010, 2015) were hypothesized to represent those areas in the most recent period, i.e., 2000–2002, 2003–2007, 2008–2012, and 2013–2015, respectively (D. Zhou et al., 2015, 2016).

3.2. $PM_{2.5}$ concentration difference

The annual mean $PM_{2.5}$ concentration dataset (website: http://fizz.phys.dal.ca/~atmos/martin/, spatial resolution: 1 km) was estimated by combining aerosol optical depth (AOD) retrievals from the Moderate Resolution Imaging Spectroradiometer (MODIS), the Multi-angle Imaging SpectroRadiometer (MISR), and the Sea-viewing Wide Field-of-view Sensor (SeaWiFS) instrument. For each satellite source, the total column retrievals of AOD were related to near-ground $PM_{2.5}$ using the Goddard Earth Observing System chemical (GEOS-Chem) transport model (Van Donkelaar et al., 2010), and were then calibrated to global ground-based observations of $PM_{2.5}$ by geographically weighted regression (GWR) (Boys et al., 2014; Van Donkelaar et al., 2015, 2016). The datasets were highly consistent with the ground measurement (R^2 = 0.81), which hence endorses the rationality of the application of this

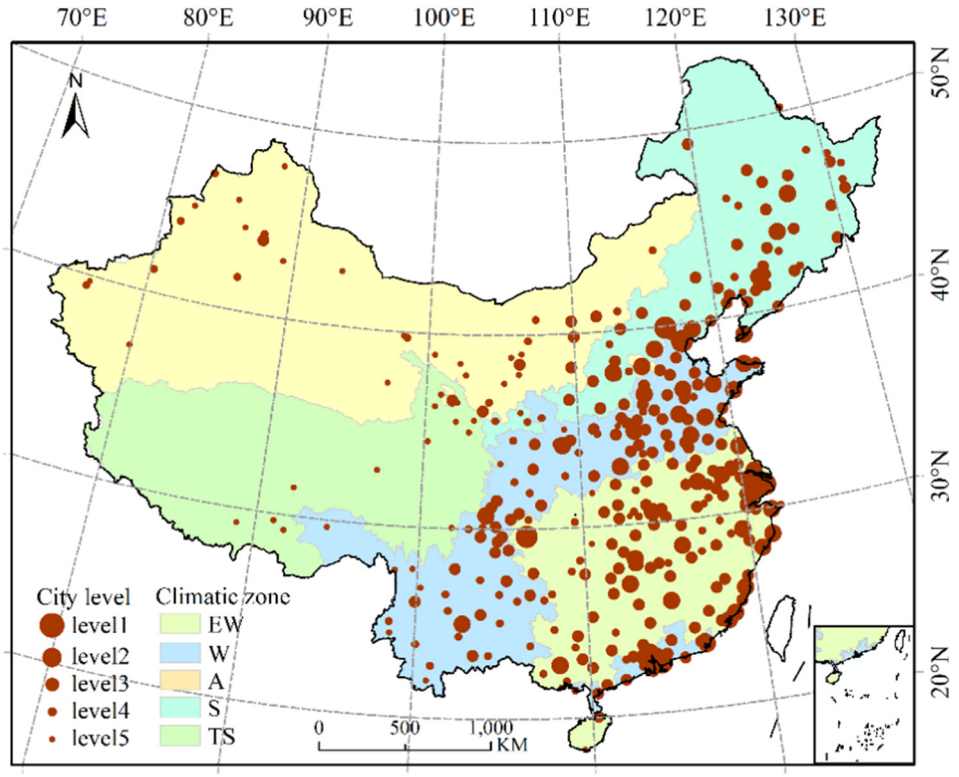

Fig. 1. Locations of the 338 prefectures with different city levels and climatic zones in China. The five colors represent the five climatic zones (i.e. equatorial and warm (EW), warm (W), arid (A), snow (S), and tundra and snow (TS)). The circles with different sizes indicate the five city levels, with the larger size corresponding to a higher city level in terms of population. This map was generated using ArcGIS 10.0 software (www.esri.com/software/arcgis).

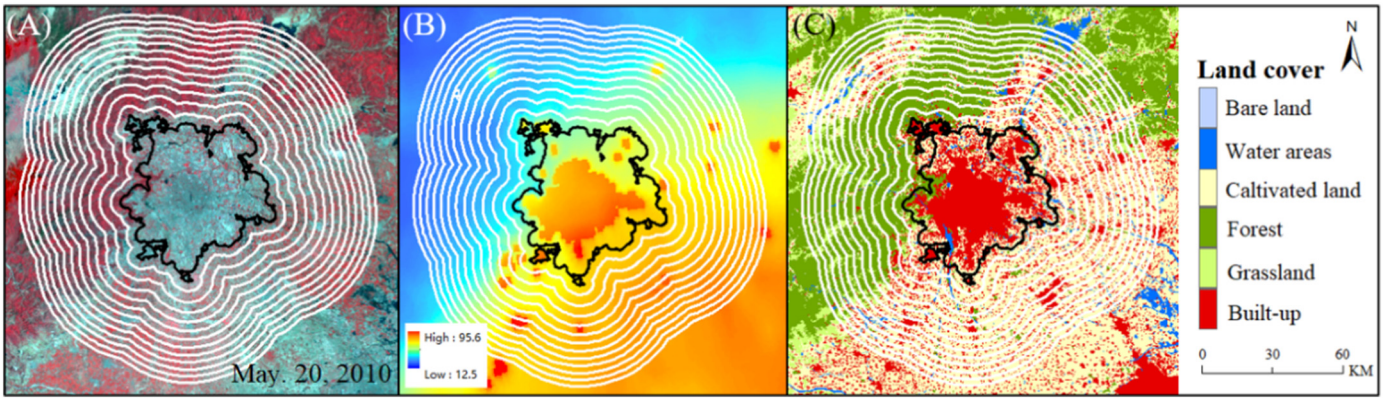

Fig. 2. The delineation of the urban area and the 12 buffer zones, using Beijing as an example. (A) Landsat Thematic Mapper false color image in May 20, 2010. (B) Annual average $PM_{2.5}$ concentration in 2010. (C) Land-cover map from the CLUD for 2010, with a spatial resolution of 30 m. The black line represents the border of the urban area, and the land within the border is regarded as the urban area. The white lines represent the border of the buffers (the area for each of them is set to half the urban area). The maps were generated using ArcGIS 10.0 (www.esri.com/software/arcgis).

dataset. A subset covering China from 2000 to 2015 was adopted in this study.

For each city, ΔC_i, defined as the $PM_{2.5}$ concentration difference between the i-th buffer area C_i and background area C_b, was calculated with the following equation:

$$\Delta C_i = C_i - C_b, C_b = median(C_{10}, C_{11}, C_{12}), \quad i = \{0 \ldots 12\} \tag{1}$$

where C_0 represents the $PM_{2.5}$ concentration in the urban area, and C_b is the median of the mean $PM_{2.5}$ concentration in the natural background (i.e., the last three buffer zones), representing the pollution intensity of the background. The reason for taking the median value is to reduce the bias due to the possible outlier in the three farthest buffer zones. ΔC is the set of differential values for all the buffer zones (i.e., a series of ΔC_i values). To examine the trend of ΔC for each city, an exponential decay model was utilized:

$$\Delta C_i = A \times e^{-\frac{1}{2} \times s \times i} + C_a, \quad i = \{0 \ldots 12\} \tag{2}$$

where i, the indicator of current buffer zones, represents the distance from the urban area (i.e., 12 buffer zones emanating outward from the urban area were gradually generated, with each covering half the size of the urban area), A indicates the maximum concentration difference, s is the decay rate, and C_a is the asymptotic value of the exponential trend. F-tests ($p = 0.05$) were conducted to determine whether the exponential trend of ΔC in each city was significant (i.e., the existence of the UPI phenomenon).

3.3. Metrics of UPI: UPII and UPIFP

For the cities with the UPI phenomenon, two metrics were defined to quantitatively delineate the UPI effect and its spatiotemporal pattern. Firstly, UPII (UPI intensity), which reflects the magnitude of the UPI effect, can be formulated as:

$$UPII = C_0 - C_b. \tag{3}$$

It is a well-known fact that urban pollution are from both natural and anthropogenic sources (Zhang et al., 2015), in this study, UPII measures the urban pollution level caused by anthropogenic activities by removing the influence of the natural background. According to the annual mean threshold for $PM_{2.5}$ (including both natural and anthropogenic sources) from the World Health Organization (WHO) (i.e., 10 μg/m^3), cities with $C_0 > 10$ μg/m^3 and UPII > 5 μg/m^3 (i.e., half of 10 μg/m^3) are considered as ones with a high UPII. The second metric, UPIFP (UPI footprint), quantifies the continuously affected extent from urban to background area, under the condition that ΔC is 5% larger than C_a (i.e., the asymptotic value of the exponential trend), which is a similar metric to the definition of the urban heat island extent (Zhang et al., 2004). UPIFP represents areas that are prominently affected by the UPI effect, including both urban and surrounding buffer areas, ranging from 1 to 7 times the urban area. A high value of UPIFP signifies strong pollution transfer from the urban area to its surrounding areas. In other words, the smallest UPIFP value indicates very weak pollution transmission from the urban area to its surrounding areas, and the pollution is concentrated in the urban area only. Meanwhile, the largest UPIFP value means that the urban pollution is transported to the furthest buffer zone (i.e., the 12th buffer in this study) and spreads to seven times the urban area. In this study, cities with a UPIFP value greater than the median value (i.e., four times the urban area) were classified as the ones with a large range of affected extent. In addition, both metrics were marked as null for the cities without UPI effects.

3.4. Spatiotemporal patterns of the UPI effect

Based on the UPII and UPIFP values, statistics on their annual average can give us a glimpse of the pollution situation at a national scale. In addition, the differences across city levels and climatic zones, tested by one-way analysis of variance (ANOVA) and Fisher's least significant difference (LSD), can measure the variations of UPI across different groups of cities. Subsequently, linear trend analysis was used to explore the temporal dynamics of the UPI effect during 2000–2015, including the overall trend and across different city levels and climatic zones. The unary linear model is defined as:

$$UPI_j = K \times j + B, \quad j = \{2000 \ldots 2015\} \tag{4}$$

where UPI_j is the UPII (or UPIFP) in the year of j, K represents the change rate of UPII (or UPIFP), and B is the bias term in each model. F-tests ($p = 0.05$) were conducted to determine whether the linear trend of UPI was significant.

4. Results and discussion

4.1. The existence of UPI and correlation with land use/cover

To explore the existence of the UPI effect over the study period, we measured the trends of ΔC from urban to background areas. Visually, ΔC of cities in various levels and climatic zones show exponential decreasing trends (Fig. 3). For instance, Beijing (Fig. 3 and Table S1), the

capital of China, displays an exponentially declining trend of annual average ΔC, with the maximum concentration difference (i.e., *A*, a close value of UPII) reaching 13.83 ± 0.77 μg/m^3. When taking all 338 cities into account, ΔC declines exponentially as a function of distance (*i*) to the urban areas: $\Delta C = 3.91 \times e^{-\frac{1}{2}\times 1.99\times i} + 0.17$, with $R^2 = 0.98$, $p < 0.01$. In total, 84% (283 of 338) of the cities show exponentially decreasing trends of ΔC from urban to background areas averaged over 2000–2015, and 63% (214/338) of the cities showed the trends during the whole sixteen-year period (Table S1). These results verify the existence of the UPI phenomenon, i.e., higher particle concentrations in urban areas are gradually attenuated to background areas.

Previous studies have reported that $PM_{2.5}$ pollution levels correspond to various land-use/cover types (Han et al., 2015). Here we analyzed the direct affection from land-cover, that is, in view of built-up (vegetation) proportion in the study areas. In this study, pixels that were labeled as grass land or forest in CLUDs (China Land Use/Cover Datasets) are considered as vegetation areas, and those are labeled as built-up are regarded as built-up areas. Specifically, the average built-up (vegetation) proportion in the urban and background areas in all the study cities in 2015 were 43% ± 12% (18% ± 18%) and 8% ± 7% (39% ± 28%), respectively, accounting for the remarkable concentration differences between urban and background areas. Several studies, based on the ground measurements, have indicated the impact of land-use/cover density on pollution patterns within urban areas (Weng and Yang, 2006; Xian, 2007). For example, Weng and Yang (2006) found that, in Guangzhou, the ground monitoring stations which are far away from the city center or road showed low pollution concentrations. Xian (2007) revealed that higher pollution concentrations can be observed in regions with higher urban development intensity (i.e., a higher percentage of anthropogenic impervious surfaces) in urban land in Las Vegas. Nonetheless, pollution concentration distribution from urban areas to their surrounding areas (spatial concentration trend), as well as the relationship with land-use/cover patterns, has not been considered in previous studies. In this research, we found that the $PM_{2.5}$ pollution level rises with the increment of the anthropogenic land-use density (i.e., the built-up proportion) and demonstrates an increasing trend toward the city centers (Fig. 4). An urban-background gradient exists in the concentration of $PM_{2.5}$, and the UPI phenomenon is therefore captured.

In the meantime, there are still 37% (124/338, Table S1) of the cities with an evident UPI effect during several years or without UPI during study period, which can be categorized into four situations. For the first situation, the UPI phenomenon was captured in 3% (10/338) of the cities only in the first few years of the study period, due to the abrupt land-use/cover change in the subsequent years. Taking Jinan (in the W2 region) as an example, a significant UPI effect can be observed before

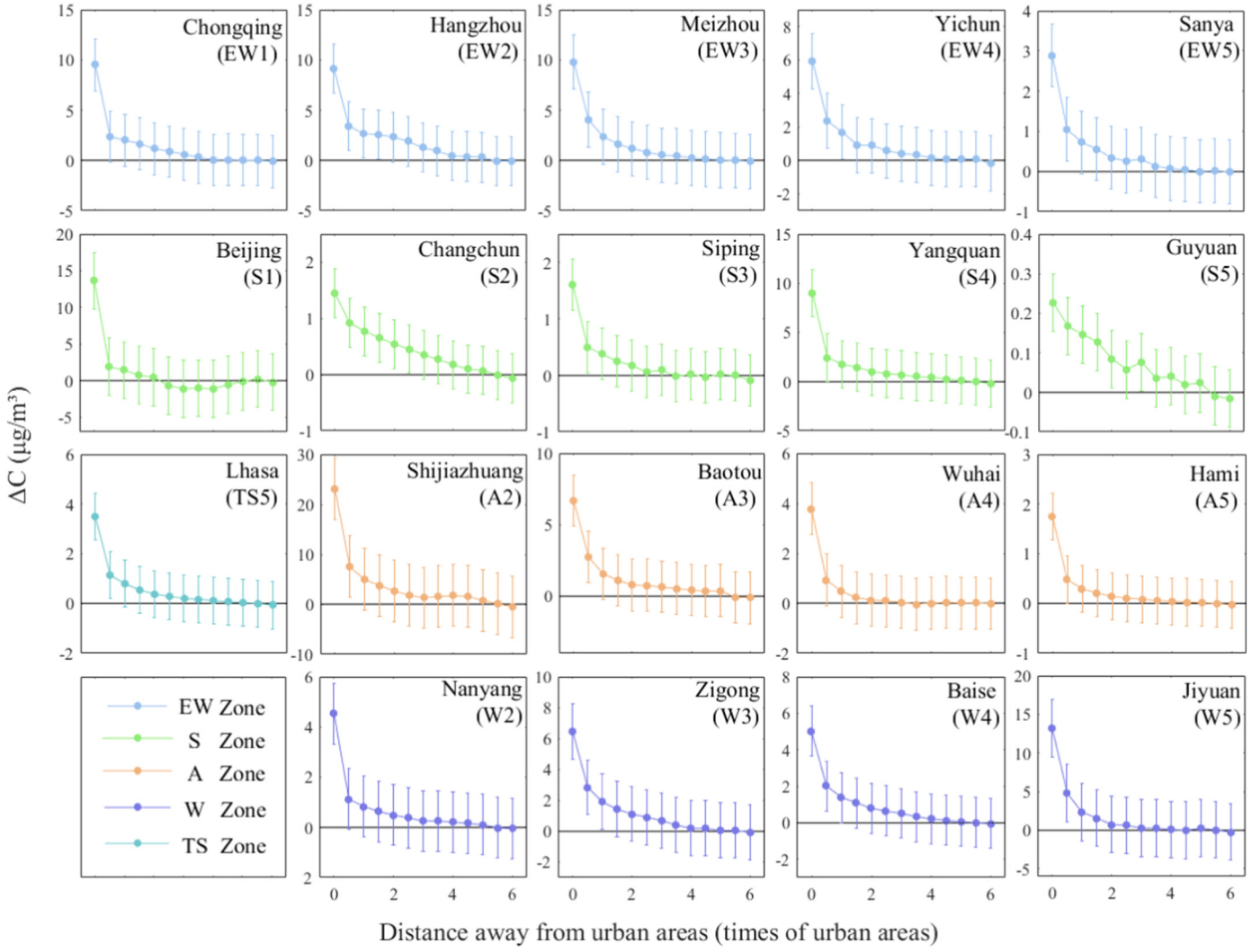

Fig. 3. Trends of ΔC from urban to background areas averaged over 2000–2015 for several example cities in different city levels and climatic zones. The capital letters EW, S, A, TS, and W represent the five corresponding climatic zones (i.e. equatorial and warm (EW), snow (S), arid (A), tundra and snow (TS) and warm (W)). The numbers 1, 2, 3, 4, and 5 represent the five corresponding city levels, i.e., super city, mega city, large city, medium city, and small city, respectively. The error bars are the standard deviation.

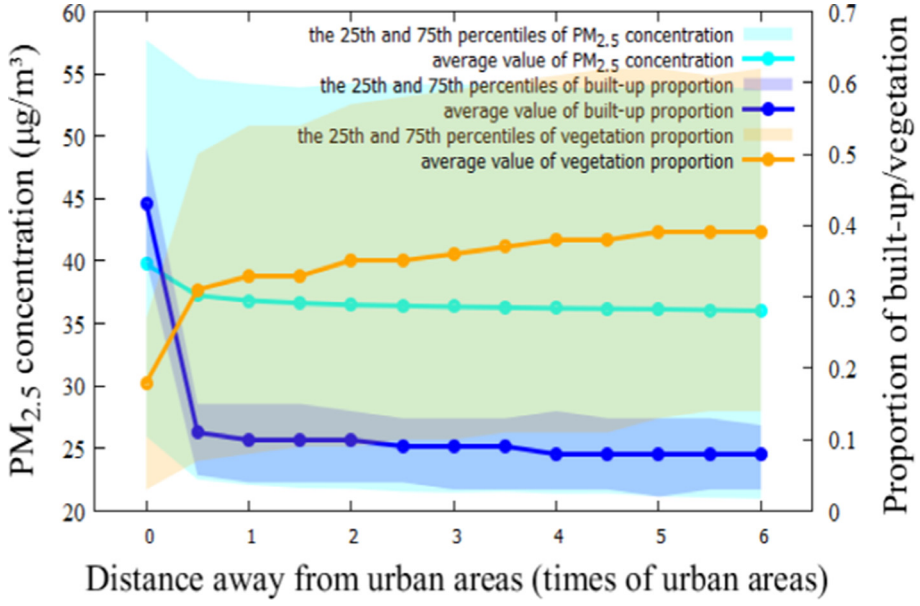

Fig. 4. $PM_{2.5}$ concentration and the proportions of built-up and vegetation from urban to background areas (in 2015).

2007. However, after 2007, a large amount of scattered built-up areas appeared in the urban-rural fringes during the rapid urbanization, leading to a decrease or even disappearance of the UPI phenomenon (Fig. 5A). In the second situation, in contrast, 1% (4/338) of the cities showed an evident UPI effect in the later years, due to the gradually increasing land-use/cover difference between urban and neighboring areas. For example, before 2012, in Shuangyashan, the urban center was surrounded by several villages and towns. However, from 2013 to 2015, rapid expansion of the built-up areas in the city center directly led to the occurrence of the significant UPI phenomenon from 2013 (Fig. 5B). For the third situation, the UPI effect appeared occasionally in 24% (80/338) of the cities during 2000–2015, most of which are coastal cities such as Nantong (in the EW2 region, Fig. 5C). The coastal cities can be affected by the land–sea breeze, as the distribution of $PM_{2.5}$ concentration is associated with the distance to the sea (C. Liu et al., 2016). For the fourth situation, 9% (30/124) of the cities did not show UPI in any of the years, most of which are undeveloped cities such as Nyingchi (in the W5 region, Fig. 5D). The situations of the undeveloped cities are possibly due to their small urban areas and inconspicuous concentration differences between urban and background areas (Han et al., 2014).

In summary, the UPI phenomenon can be witnessed nationwide in recent years, owing to the difference of land-use/cover patterns between urban and surrounding areas, under the context of rapid

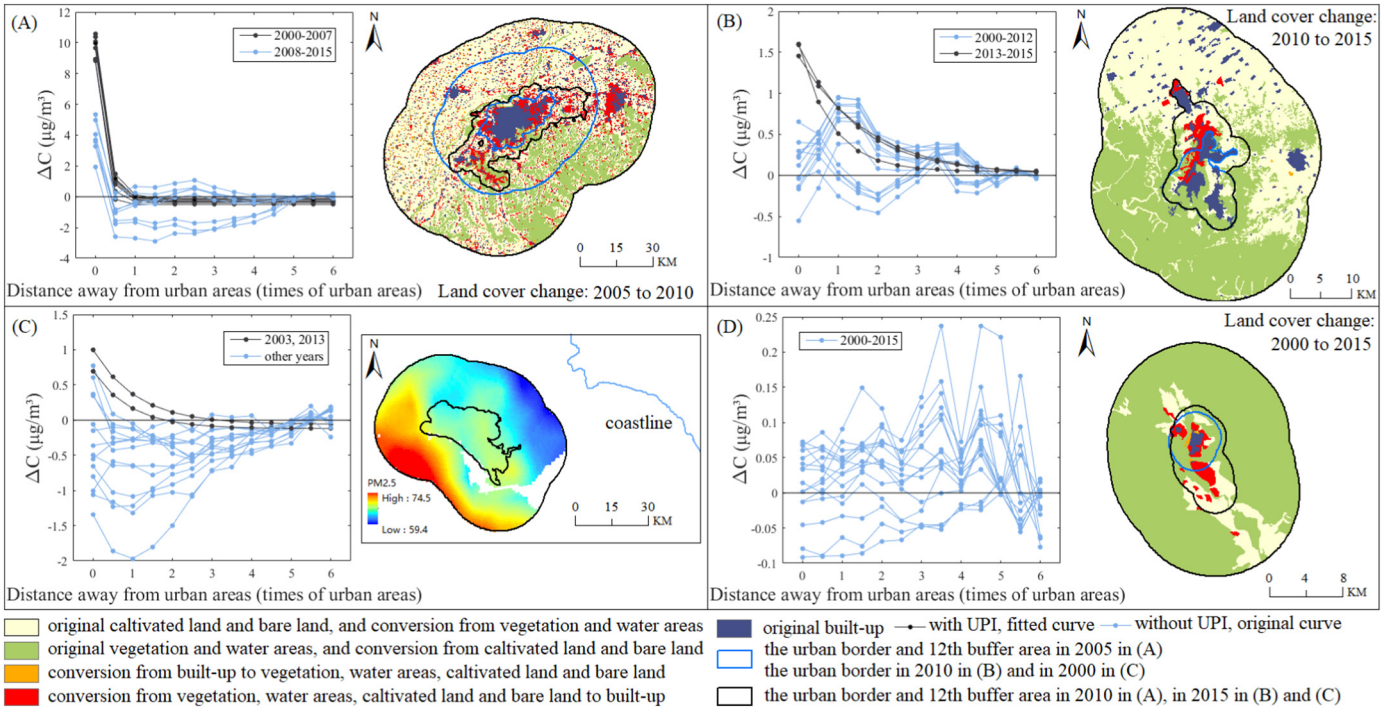

Fig. 5. Cities with an evident UPI effect in a couple of years or without UPI during 2000–2015, using Jinan (A), Shuangyashan (B), Nantong (C), and Nyingchi prefecture (D) as examples.

urbanization. Despite the efforts made in air pollution control, the large amount of pollution emissions in built-up areas during the rapid urbanization can cause the higher $PM_{2.5}$ concentrations in urban areas than their surrounding areas (Bressi et al., 2013). The existence of the UPI phenomenon in most cities demonstrates the dominant role of emissions for affecting the distribution of $PM_{2.5}$ pollution. Our findings will provide scientific evidence for urban air pollution control in different cities, and will also provide a comprehensive reference to balancing urbanization and environmental protection for other rapid urbanization regions/countries.

4.2. Spatial analysis of UPII and UPIFP

By averaging the $PM_{2.5}$ concentration data over 2000–2015, the magnitude and the extent of the UPI effect were measured to reflect the overall $PM_{2.5}$ pollution status of China (Fig. 6). Overall, there are 283 cities with an evident UPI phenomenon (see Table S1 in Supplementary materials for the exponential modeling results of each city), and the other 55 cities which do not show the UPI phenomenon are mainly located in western China, environmental protection regions, and coastal areas. During 2000–2015, China suffered from a severe UPI problem. Concerning UPII, the values of nearly half of the cities (120/283) are larger than 5 μg/m^3, illustrating the serious urban pollution induced by human activities. These prefectures are mainly located in the BTH (Beijing-Tianjin-Hebei) region, Zhejiang province, and Fujian province. In particular, the UPII values of seven cities in these regions, i.e., Beijing, Baoding, Shijiazhuang, Xingtai, Handan, Fuzhou, and Zhangzhou, are more than 12 μg/m^3. When looking at the values of UPIFP, more than half of the cities (160/283) show values between 4.5 and 7, suggesting strong pollution spread in these cities. In particular, the cities with UPIFP values in the range of 6 to 7, indicating that neighborhoods of 6–7 times the urban areas are still affected by the anthropogenic emissions from the urban areas, are mainly located in northern China and the southeast coastal cities.

The UPII and UPIFP values in different city levels and climatic zones were further investigated (Fig. 7 and Table S2). Across the city levels, the UPII in cities of a higher level (i.e., more urban residents) is greater than that in those of lower levels (Fig. 7A, $F = 5.822$, $p < 0.001$), while there is no significant difference in UPIFP across the different city levels (Fig. 7C, $F = 0.575$, $p = 0.681$). For instance, the UPII in the super cities (i.e., Level 1) is significantly higher than that in the large, medium, and small cities (Level 3: $p < 0.05$, Level 4: $p < 0.05$ and Level 5: $p < 0.01$). Such results indicate that aggregated urban population can increase urban pollution levels, but cannot directly affect the diffusion of the urban pollution. In view of climatic zones, cities in eastern China (the EW, W, and S zones) experience a significantly higher UPII (Fig. 7B, $F = 2.567$, $p < 0.05$), while cities in the EW and A zones have a higher UPIFP (Fig. 7D, $F = 4.951$, $p < 0.01$). In detail, UPII in the TS zone is significantly lower than that in the EW, W, and S zones (EW zone: $p < 0.05$, W zone: $p < 0.05$ and S zone: $p < 0.01$). This reveals that the cities with more rapid urbanization in eastern China tend to have high UPII, but UPIFP appears sensitive to regional meteorological conditions, since significant differences can be captured among the different climatic zones but not among the different city levels.

In terms of the distribution characteristics, the spatial patterns of the UPI effect can be divided into the following categories. Firstly, a high UPII but small UPIFP, are found in BTH (Beijing-Tianjin-Hebei) (Fig. 6). As a result of the massive urban pollution emissions (Wang et al., 2013) and unfavorable dispersion conditions (weak wind and low boundary layer height) (Miao et al., 2015), $PM_{2.5}$ pollution concentrates in the urban areas and has difficulty diffusing to the surrounding areas, which is consistent with the previous findings of Zhang and Cao (2015). Meanwhile, the large difference in built-up proportion between the urban and suburban areas can amplify the energy gradient (Sherwood, 2002; Offerle et al., 2005), and aggravate the decay of air pollutants and further dwarf UPIFP (Table S3).

Secondly, the cities in northern China, the PRD (Pearl River Delta) and YRD (Yangtze River Delta) show moderate UPII values but large UPIFP values (Fig. 6). Previous works focusing on $PM_{2.5}$ concentration

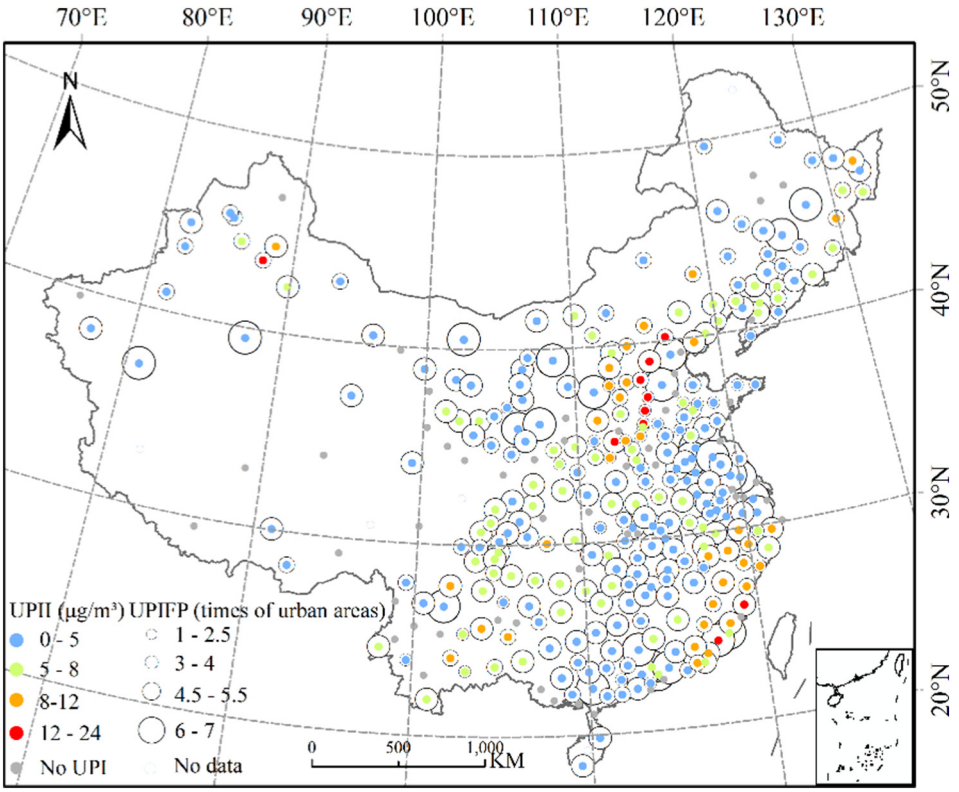

Fig. 6. Spatial distribution of the UPI effect averaged over 2000–2015. The map was generated using ArcGIS 10.0 software (www.esri.com/software/arcgis).

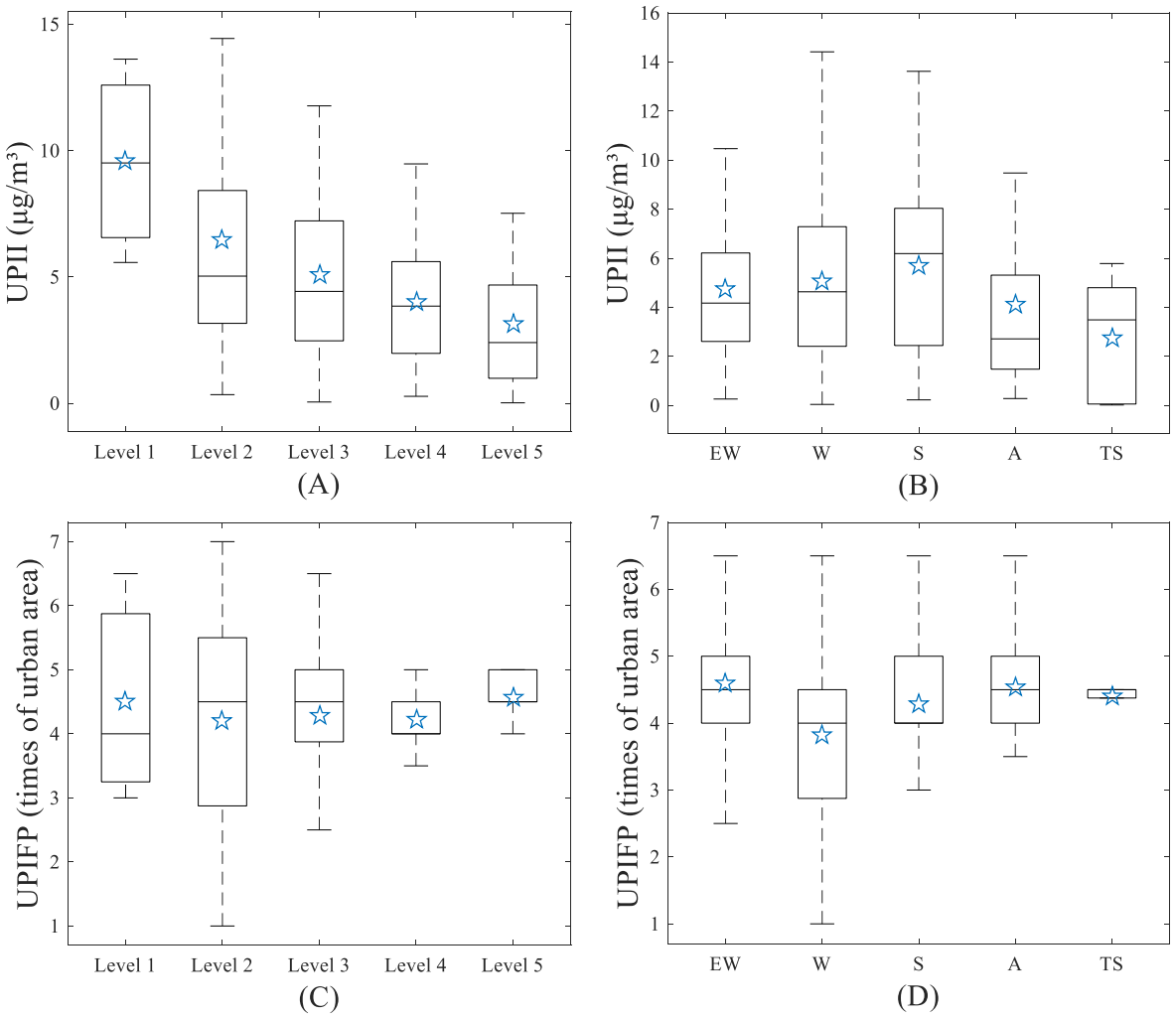

Fig. 7. UPII (A and B) and UPIFP (C and D) averaged over 2000–2015 for different city levels and climatic zones. Abbreviations of the city levels: super city (Level 1), mega city (Level 2), large city (Level 3), medium city (Level 4), and small city (Level 5). The boxes represent the 25th and 75th percentiles, with the whiskers extending to the minimum and maximum values. The central lines in the boxes are the median values, and the blue pentagrams represent the mean values.

at the whole city scale (i.e., including both the urban area and its background) have reported severe pollution in northern China (Y.G. Wang et al., 2014; He et al., 2017), whereas a moderate UPII, which indicates a low urban pollution level (especially in the underdeveloped regions, e.g., Xinjiang and Inner Mongolia), is observed in this study. The results suggest less anthropogenic pollution in the urban areas and a high contribution of the pollution in surrounding areas to the pollution in the cities, which is in line with the large UPIFP values in these regions. This is likely related to the transport of air pollutants by the frequent sandstorms and the sparse vegetation cover (Xu et al., 2006; Salmond et al., 2013). For cities in the PRD and YRD, the sea breeze can transfer air pollutants from the coastal cities to the adjacent cities (Ding et al., 2004; H. Wang et al., 2014). This pollution transfer dilutes the urban $PM_{2.5}$ concentration and/or disrupts the pollution distribution (Wu et al., 2015), causing the weak or non-obvious UPI effect in several coastal cities. Simultaneously, the pollution from these cities is transported to the surrounding areas of adjacent coastal cities, which decreases the concentration difference between the urban and background areas in the adjacent cities, leading to the moderate UPII.

Notably, both high UPII and UPIFP are observed in the WTS (Western Taiwan Straits) region. Benefiting from the government support, advantageous geographical location and abundant resources, this region has been undergoing accelerated urbanization (Z. Niu et al., 2013; Yin et al., 2014). Increasing local emissions, such as those caused by transportation of port cargos are found (Lu et al., 2014; Wu et al., 2015), accounting for the high UPII. In addition to the severe urban pollution, the high UPIFP is also observed, illustrating the strong transmission of the urban pollution to their surrounding areas. Besides, under the influence of the East Asian monsoon circulation characterized by south-southwest wind in summer and north-northeast wind in the other three seasons, air pollutants from adjacent developed regions (i.e., PRD and YRD) can be transported to the WTS region (Hsu et al., 2010; Yang et al., 2011), aggravating the overall pollution. However, compared with the other rapidly developing regions, studies of $PM_{2.5}$ pollution in the WTS region are scarce (Xu et al., 2013). In consideration of both the severe urban pollution and the wide range of affected areas, more attention should be paid to this region in the future.

Given the different spatial patterns of the UPI effect, specific control measures should be adopted across the diverse regions. In the BTH region, where there is high urban pollution, but relatively small-sized affected areas, attention should be paid to the urban core areas. In addition to the stringent emission control policies in urban areas (Zhang et al., 2016), urban landscape configuration may also help to mitigate the high UPII in this region (Bandeira et al., 2011; Larkin et al., 2016). For instance, cities with highly compact built-up areas tend to have lower urban $PM_{2.5}$ pollution levels, since the more convenient commuting and available mass-transit systems in geometrically compact cities can help to reduce vehicle emissions (Marshall et al.,

2005). Moreover, our research demonstrates that, for the cities with large UPIFP in northern China, it is possible to reduce the spread of urban pollution by increasing the vegetation cover in the suburban areas. For cities in southeastern China, most of the coastal cities generally exhibit evident UPI effects, and show diverse UPI patterns due to the different characteristics of the sea breeze. Considering that the sea breeze in coastal regions can either worsen or improve regional air quality by trapping or diluting air pollutants (Baumgardner et al., 2006), it can also affect the pollution distribution, and is conductive to reducing the UPI effect in some coastal cities. In view of the wide range of affected surrounding areas in the PRD, YRD, and WTS, study of the complex effect of sea breeze on pollution diffusion will be necessary in further research.

4.3. Temporal trends of the UPI effect

The UPI dynamics in the cities (184/338) with an evident UPI effect throughout 2000 to 2015 were explored in this study. Both UPII and UPIFP show significant decreasing trends from 2000 to 2015, with average annual decrease of 0.11 ± 0.01 μg/m^3·year and 0.01 ± 0.003 times the urban area/year, respectively (Fig. 8A, $R^2 = 0.88$, $p < 0.01$; Fig. 8B, $R^2 = 0.65$, $p < 0.01$). The national averaged UPII and UPIFP were 6.62 ± 3.90 μg/m^3 and 4.36 ± 0.94 times in 2000, but decreased to 5.40 ± 3.24 μg/m^3 and 4.19 ± 1.17 times by 2015. The results illustrate the overall mitigation of the UPI effect. Focusing on the temporal trends of $PM_{2.5}$ concentration, previous studies have explored the impact of human activities during urbanization on air pollution (Hsu et al., 2012; Boys et al., 2014; Ma et al., 2014; Peng et al., 2016). However, these results are affected by the pollution in the natural background or surrounding environments, such as biomass burning emissions (Granier et al., 2011). In this work, we aim to analyze the urban pollution induced by human activities, without the influence of the natural background, through the UPI phenomenon. In contrast to the overall increasing trend of $PM_{2.5}$ concentration found in previous studies (Ma et al., 2014; Peng et al., 2016), the findings of this study suggest the reduction of urban pollution in China. In addition, the reduced extent and intensity of the urban pollution were revealed in this study for the first time.

Considering the impact of land use/cover on pollution concentration distribution and the UPI phenomenon, land-use/cover change, as a direct impact of urbanization (Li et al., 2013; Fu and Weng, 2016), is an essential factor for the mitigation of UPI. As vegetation is conducive to reduce the pollution level (Nowak et al., 2006; Salmond et al., 2013), increase of urban vegetation coverage may contributed to the mitigation of UPI. In particular, the urban vegetation areas in cities with the UPI effect has increased by 16.09 ± 23.71 km^2 on average from 2000 to 2015, which may be responsible for the reduction of urban pollution. Although a large proportion of artificial surfaces in urban areas have shown significant increasing trends of $PM_{2.5}$ concentration (Han et al., 2015), the UPII mitigation observed in our study indicates that intensified human activities during urbanization does not necessarily exacerbate overall urban $PM_{2.5}$ pollution. Furthermore, our results convey the information that larger urban expansion rates (derived from CLUD data) and urban population are related to steeper decline of UPII in China during 2000–2015 (Figs. 9A and S1). In addition to the more stringent emissions controls (Dong et al., 2013), this result may also be attributed to the better development of urban green spaces in these cities (Zhao et al., 2013).

Meanwhile, similar to the fact that strong land-use/cover differences between urban and surrounding areas can amplify the energy gradient and decrease the areas affected by the UHI effect (Offerle et al., 2005; Zhou et al., 2014b), a large difference can also aggravate the decay of air pollutants (Sherwood, 2002). Our results show that the built-up proportion in the urban and suburban areas increased from 32% ± 10% and 7% ± 5% to 42% ± 10% and 10% ± 6%, respectively, during 2000–2015, corresponding to an increase of the built-up proportion difference between urban and suburban areas from 25% ± 7% to 32% ± 7% (Table S4), which indicates the potential contribution to the increase of the decay rate and the decline of UPIFP. As a conclusion, the increased urban green spaces and built-up proportion differences between urban and suburban areas during urbanization contribute to the UPI mitigation, including both the reduction of urban pollution levels, as well as the affected areas.

5. Conclusions

The urban particulate matter island (UPI) effect, which refers to the phenomenon that higher particle concentrations in urban areas are gradually attenuated to background areas, was first defined and investigated in this paper. Based on observations from 338 Chinese prefectures during 2000–2015, we explored the existence of the UPI effect, and further investigated its spatiotemporal patterns across different city levels and climatic zones. The following conclusions were made:

1) There is an evident UPI effect in China nationwide, owing to the difference in land-use/cover patterns between urban areas and surrounding areas under the context of rapid urbanization. In addition, the UPI phenomenon found in this study can be viewed as an important reference for other countries undergoing rapid urbanization.
2) During 2000–2015, China suffered a severe UPI problem, and showed different spatial patterns, i.e., high UPII but small UPIFP in

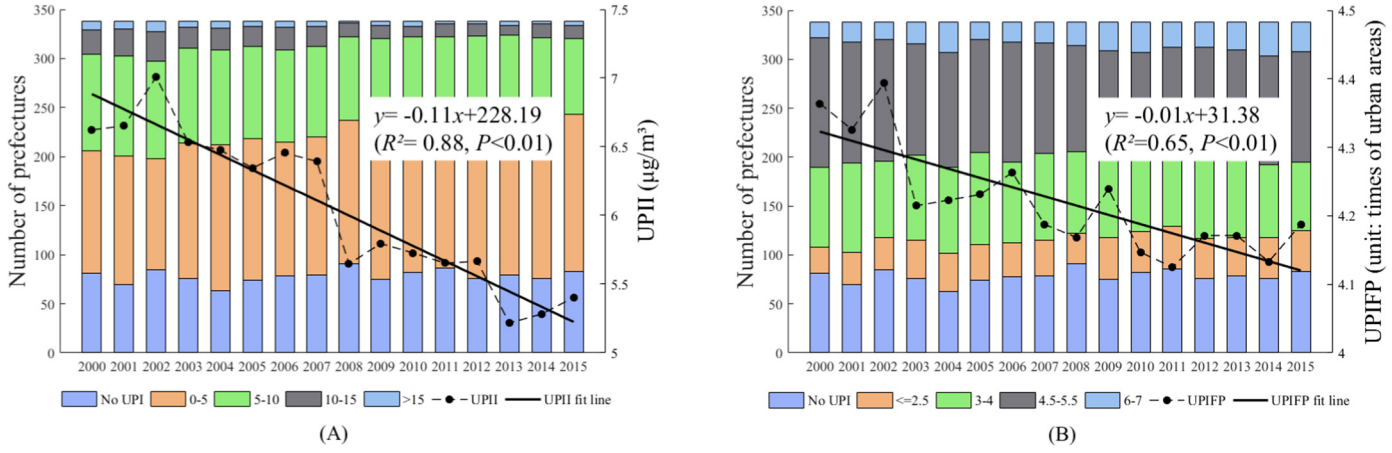

Fig. 8. UPII (A) and UPIFP (B) dynamics during 2000–2015. The dots represent average UPII (UPIFP) for the 184 cities with an evident UPI effect in every year. The lines were obtained by linear fitting.

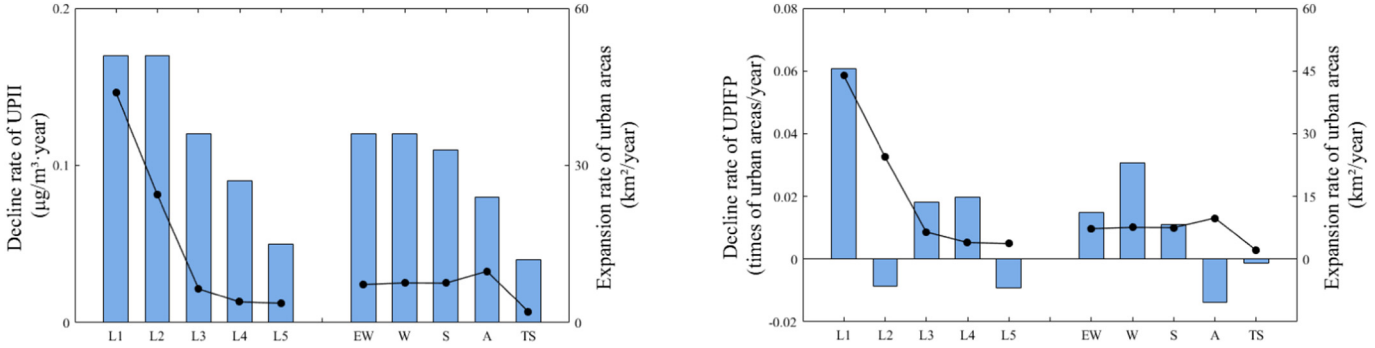

Fig. 9. Urban expansion rate and UPI decrease rate (UPII (A) and UPIFP (B)) in the different city levels and climatic zones from 2000 to 2015. The bars represent the UPII (UPIFP) decrease rate, and the lines represent the urban expansion rate. Cities with a significant UPI effect during the whole study period are considered.

the Beijing-Tianjin-Hebei, moderate UPII but large UPIFP in northern China, the Pearl River Delta and the Yangtze River Delta, and both high UPII and UPIFP in the Western Taiwan Straits region. Specific measures should be taken in different regions, to mitigate the magnitude and extent of $PM_{2.5}$ pollution.

3) UPI mitigation can be seen nationwide, with significant decreasing trends of both UPII and UPIFP, benefiting from the increase in urban green spaces and the built-up proportion differences between urban and suburban areas during urbanization. Additionally, cities with more urban residents and faster urban expansion tend to show steeper decline of UPII in China during 2000–2015, which can be primarily attributed to the greater positive effects derived from urbanization, such as the construction of urban green spaces and more stringent emission control efforts.

Acknowledgment

The research was supported by the National Natural Science Foundation of China under Grant 41701382 and 41771360, the National Program for Support of Top-notch Young Professionals, the Hubei Provincial Natural Science Foundation of China under Grant 2017CFA029, and the National Key R&D Program of China under Grant 2016YFB0501403.

Appendix A. Supplementary data

Supplementary data to this article can be found online at https://doi.org/10.1016/j.scitotenv.2019.01.099.

References

Aldabe, J., Elustondo, D., Santamaría, C., et al., 2011. Chemical characterisation and source apportionment of PM2.5 and PM10 at rural, urban and traffic sites in Navarra (North of Spain). Atmos. Res. 102 (1–2), 191–205.
Angel, S., Parent, J., Civco, D.L., et al., 2011. The dimensions of global urban expansion: estimates and projections for all countries, 2000–2050. Prog. Plan. 75 (2), 53–107.
Bandeira, J.M., Coelho, M.C., Sá, M.E., et al., 2011. Impact of land use on urban mobility patterns, emissions and air quality in a Portuguese medium-sized city. Sci. Total Environ. 409 (6), 1154–1163.
Baumgardner, D., Raga, G.B., Grutter, M., et al., 2006. Evolution of anthropogenic aerosols in the coastal town of Salina Cruz, Mexico: part I particle dynamics and land–sea interactions. Sci. Total Environ. 367 (1), 288–301.
Bellander, T., Berglind, N., Gustavsson, P., et al., 2001. Using geographic information systems to assess individual historical exposure to air pollution from traffic and house heating in Stockholm. Environ. Health Perspect. 109 (6), 633.
Boys, B.L., Martin, R.V., Van Donkelaar, A., et al., 2014. Fifteen-year global time series of satellite-derived fine particulate matter. Environ. Sci. Technol. 48 (19), 11109–11118.
Bressi, M., Sciare, J., Ghersi, V., et al., 2013. A one-year comprehensive chemical characterisation of fine aerosol (PM2.5) at urban, suburban and rural background sites in the region of Paris (France). Atmos. Chem. Phys. 13 (15), 7825–7844.
Crutzen, P.J., 2004. New directions: the growing urban heat and pollution "island" effect-impact on chemistry and climate. Atmos. Environ. 38 (21), 3539–3540.
Cumming, G.S., Buerkert, A., Hoffmann, E.M., et al., 2014. Implications of agricultural transitions and urbanization for ecosystem services. Nature 515, 50–57.
Ding, A., Wang, T., Zhao, M., et al., 2004. Simulation of sea-land breezes and a discussion of their implications on the transport of air pollution during a multi-day ozone episode in the Pearl River Delta of China. Atmos. Environ. 38 (39), 6737–6750.
Dong, X., Gao, Y., Fu, J., et al., 2013. Probe into gaseous pollution and assessment of air quality benefit under sector dependent emission control strategies over megacities in Yangtze River Delta, China. Atmos. Environ. 79, 841–852.
Fu, P., Weng, Q., 2016. A time series analysis of urbanization induced land use and land cover change and its impact on land surface temperature with Landsat imagery. Remote Sens. Environ. 175, 205–214.
Granier, C., Bessagnet, B., Bond, T., et al., 2011. Evolution of anthropogenic and biomass burning emissions of air pollutants at global and regional scales during the 1980–2010 period. Clim. Chang. 109 (1–2), 163.
Grimm, N.B., Faeth, S.H., Golubiewski, N.E., et al., 2008. Global change and the ecology of cities. Science 319 (5864), 756–760.
Han, L., Zhou, W., Li, W., et al., 2014. Impact of urbanization level on urban air quality: a case of fine particles (PM2.5) in Chinese cities. Environ. Pollut. 194, 163–170.
Han, L., Zhou, W., Li, W., 2015. City as a major source area of fine particulate (PM2.5) in China. Environ. Pollut. 206, 183–187.
He, C.Y., Han, L.J., Zhang, R.Q., 2016. More than 500 million Chinese urban residents (14% of the global urban population) are imperiled by fine particulate hazard. Environ. Pollut. 218, 558–562.
He, J., Gong, S., Yu, Y., et al., 2017. Air pollution characteristics and their relation to meteorological conditions during 2014–2015 in major Chinese cities. Environ. Pollut. 223, 484–496.
Hijmans, R., Garcia, N., Wieczorek, J., 2010. GADM: Database of Global Administrative Areas (Version).
Hoff, R.M., Christopher, S.A., 2009. Remote sensing of particulate pollution from space: have we reached the promised land? J. Air Waste Manage. Assoc. 59 (6), 645–675.
Hsu, S.C., Liu, S.C., Tsai, F., et al., 2010. High wintertime particulate matter pollution over an offshore island (Kinmen) off southeastern China: an overview. J. Geophys. Res. 115 (D17).
Hsu, N.C., Gautam, R., Sayer, A.M., et al., 2012. Global and Regional Trends of Aerosol Optical Depth over Land and Ocean Using SeaWiFS Measurements From 1997 to 2010.
Hsu, C.Y., Chiang, H.C., Chen, M.J., et al., 2017. Ambient PM2. 5 in the residential area near industrial complexes: spatiotemporal variation, source apportionment, and health impact. Sci. Total Environ. 590, 204–214.
Hua, Y., Cheng, Z., Wang, S., et al., 2015. Characteristics and source apportionment of PM2.5 during a fall heavy haze episode in the Yangtze River Delta of China. Atmos. Environ. 123, 380–391.
Kabashnikov, V., Milinevsky, G., Chaikovsky, A., et al., 2014. Localization of aerosol sources in East-European region by back-trajectory statistics. Int. J. Remote Sens. 35 (19), 6993–7006.
Karl, T.R., Trenberth, K.E., 2003. Modern global climate change. Science 302 (5651), 1719–1723.
Kong, S., Han, B., Bai, Z., et al., 2010. Receptor modeling of PM2.5, PM10 and TSP in different seasons and long-range transport analysis at a coastal site of Tianjin, China. Sci. Total Environ. 408 (20), 4681–4694.
Larkin, A., van Donkelaar, A., Geddes, J.A., et al., 2016. Relationships between changes in urban characteristics and air quality in East Asia from 2000 to 2010. Environ. Sci. Technol. 50 (17), 9142–9149.
Lelieveld, J., Evans, J.S., Fnais, M., et al., 2015. The contribution of outdoor air pollution sources to premature mortality on a global scale. Nature 525 (7569), 367.
Li, Y., Zhu, L., Zhao, X., et al., 2013. Urbanization impact on temperature change in China with emphasis on land cover change and human activity. J. Clim. 26 (22), 8765–8780.
Li, H., Wang, Q.G., Yang, M., et al., 2016. Chemical characterization and source apportionment of PM2.5 aerosols in a megacity of Southeast China. Atmos. Res. 181, 288–299.
Liu, J., Han, Y., Tang, X., et al., 2016. Estimating adult mortality attributable to PM2.5 exposure in China with assimilated PM2.5 concentrations based on a ground monitoring network. Sci. Total Environ. 568, 1253–1262.
Liu, C., Henderson, B.H., Wang, D., et al., 2016. A land use regression application into assessing spatial variation of intra-urban fine particulate matter (PM2.5) and

nitrogen dioxide (NO_2) concentrations in City of Shanghai, China. Sci. Total Environ. 565, 607–615.
Lu, S.W., Hu, Q.H., Wu, S.P., et al., 2014. Establishment of air pollutants emission inventory in the west coast of Taiwan Straits. Acta Sci. Circumst. 34, 3624–3634 (in Chinese with English Abstract).
Ma, Z., Hu, X., Huang, L., et al., 2014. Estimating ground-level PM2.5 in China using satellite remote sensing. Environ. Sci. Technol. 48 (13), 7436–7444.
Marshall, J.D., McKone, T.E., Deakin, E., et al., 2005. Inhalation of motor vehicle emissions: effects of urban population and land area. Atmos. Environ. 39 (2), 283–295.
Miao, Y., Hu, X.M., Liu, S., et al., 2015. Seasonal variation of local atmospheric circulations and boundary layer structure in the Beijing-Tianjin-Hebei region and implications for air quality. J. Adv. Model. Earth Syst. 7 (4), 1602–1626.
Niu, F., Bai, J., Yang, Z., 2013. Annual Report on Development of Small and Medium Size Cities in China. Social Science Academic Press of China, Beijing, p. 2.
Niu, Z., Zhang, F., Chen, J., et al., 2013. Carbonaceous species in PM2.5 in the coastal urban agglomeration in the Western Taiwan Strait Region, China. Atmos. Res. 122, 102–110.
Noorhosseini, S.A., Allahyari, M.S., Damalas, C.A., et al., 2017. Public environmental awareness of water pollution from urban growth: the case of Zarjub and Goharrud rivers in Rasht, Iran. Sci. Total Environ. 599, 2019–2025.
Nowak, D.J., Crane, D.E., Stevens, J.C., 2006. Air pollution removal by urban trees and shrubs in the United States. Urban For. Urban Green. 4 (3–4), 115–123.
Offerle, B., Grimmond, C.S.B., Fortuniak, K., 2005. Heat storage and anthropogenic heat flux in relation to the energy balance of a central European city centre. Int. J. Climatol. J. R. Meteorol. Soc. 25 (10), 1405–1419.
Orza, J.A.G., Cabello, M., Galiano, V., et al., 2012. The association between NAO and the interannual variability of the tropospheric transport pathways in western Europe. In: Lin, J., Brunner, D., Gerbig, C., Stohl, A., Luhar, A., Webley, P. (Eds.), Lagrangian Modeling of the Atmosphere. American Geophysical Union, Washington, D. C. https://doi.org/10.1029/2012GM001315.
Peng, J., Chen, S., Lü, H., et al., 2016. Spatiotemporal patterns of remotely sensed PM2.5, concentration in China from 1999 to 2011. Remote Sens. Environ. 174, 109–121.
Pope, C.A., Burnett, R.T., Turner, M.C., et al., 2011. Lung cancer and cardiovascular disease mortality associated with ambient air pollution and cigarette smoke: shape of the exposure-response relationship. Environ. Health Perspect. 119, 1616–1621.
Querol, X., Alastuey, A., Rodrıguez, S., et al., 2004. Levels of particulate matter in rural, urban and industrial sites in Spain. Sci. Total Environ. 334, 359–376.
Rowe, D.B., 2011. Green roofs as a means of pollution abatement. Environ. Pollut. 159 (8–9), 2100–2110.
Rubel, F., Kottek, M., 2010. Observed and projected climate shifts 1901–2100 depicted by world maps of the Köppen-Geiger climate classification. Meteorol. Z. 19 (2), 135–141.
Salmond, J.A., Williams, D.E., Laing, G., et al., 2013. The influence of vegetation on the horizontal and vertical distribution of pollutants in a street canyon. Sci. Total Environ. 443, 287–298.
Salvador, P., Artíñano, B., Querol, X., et al., 2008. A combined analysis of backward trajectories and aerosol chemistry to characterise long-range transport episodes of particulate matter: the Madrid air basin, a case study. Sci. Total Environ. 390 (2–3), 495–506.
Seto, K.C., Fragkias, M., Güneralp, B., et al., 2011. A meta-analysis of global urban land expansion. PLoS One 6 (8), e23777.
Sherwood, S., 2002. A microphysical connection among biomass burning, cumulus clouds, and stratospheric moisture. Science 295 (5558), 1272–1275.
Stohl, A., 1998. Computation, accuracy and applications of trajectories—a review and bibliography. Atmos. Environ. 32 (6), 947–966.
Stohl, A., Haimberger, L., Scheele, M.P., et al., 2001. An intercomparison of results from three trajectory models. Meteorol. Appl. 8 (2), 127–135.
United Nations, 2012. World Urbanization Prospects: The 2012 Revision. United Nations, New York.
United Nations, 2014. Department of Economic and Social Affairs, Population Division. World Urbanization Prospects: The 2014 Revision. United Nations, New York, NY.
Van Donkelaar, A., Martin, R.V., Brauer, M., et al., 2010. Global estimates of ambient fine particulate matter concentrations from satellite based aerosol optical depth: development and application. Environ. Health Perspect. 118 (6), 847–855.
Van Donkelaar, A., Martin, R.V., Brauer, M., et al., 2015. Global fine particulate matter concentrations from satellite for long-term exposure assessment. Environ. Health Perspect. 123, 135–143.
Van Donkelaar, A., Martin, R.V., Brauer, M., et al., 2016. Global estimates of fine particulate matter using a combined geophysical-statistical method with information from satellites, models, and monitors. Environ. Sci. Technol. 50, 3762–−3772.
Van Zyl, J.J., 2001. The Shuttle Radar Topography Mission (SRTM): a breakthrough in remote sensing of topography. Acta Astronaut. 48 (5–12), 559–565.
Wang, W., Ren, L., Zhang, Y., et al., 2008. Aircraft measurements of gaseous pollutants and particulate matter over Pearl River Delta in China. Atmos. Environ. 42 (25), 6187–6202.
Wang, L.T., Wei, Z., Yang, J., et al., 2013. The 2013 severe haze over the southern Hebei, China: model evaluation, source apportionment, and policy implications. Atmos. Chem. Phys. Discuss. 13 (11).
Wang, Y.G., Ying, Q., Hu, J.L., et al., 2014. Spatial and temporal variations of six criteria air pollutants in 31 provincial capital cities in China during 2013–2014. Environ. Int. 73, 413–422.
Wang, H., An, J., Shen, L., et al., 2014. Mechanism for the formation and microphysical characteristics of submicron aerosol during heavy haze pollution episode in the Yangtze River Delta, China. Sci. Total Environ. 490, 501–508.
Weng, Q., Yang, S., 2006. Urban air pollution patterns, land use, and thermal landscape: an examination of the linkage using GIS. Environ. Monit. Assess. 117 (1–3), 463–489.
World Urbanization Prospects (2014 Revision). United Nations Department of Economic and Social Affairs, New York.
Wu, J.G., 2008. Making the case for landscape ecology: an effective approach to urban sustainability. Landsc. J. 27 (1), 41–50.
Wu, J., Jenerette, G.D., Buyantuyev, A., et al., 2011. Quantifying spatiotemporal patterns of urbanization: the case of the two fastest growing metropolitan regions in the United States. Ecol. Complex. 8 (1), 1–8.
Wu, S.P., Schwab, J., Yang, B.Y., et al., 2015. Two-years PM2.5 observations at four urban sites along the coast of southeastern China. Aerosol Air Qual. Res. 15, 1799–1812.
Xian, G., 2007. Analysis of impacts of urban land use and land cover on air quality in the Las Vegas region using remote sensing information and ground observations. Int. J. Remote Sens. 28 (24), 5427–5445.
Xu, X., Levy, J.K., Zhaohui, L., et al., 2006. An investigation of sand–dust storm events and land surface characteristics in China using NOAA NDVI data. Glob. Planet. Chang. 52 (1–4), 182–196.
Xu, L., Yu, Y., Yu, J., et al., 2013. Spatial distribution and sources identification of elements in PM2.5 among the coastal city group in the Western Taiwan Strait region, China. Sci. Total Environ. 442, 77–85.
Xu, L., Batterman, S., Chen, F., et al., 2017. Spatiotemporal characteristics of PM2.5 and PM10 at urban and corresponding background sites in 23 cities in China. Sci. Total Environ. 599, 2074–2084.
Yang, F., Tan, J., Zhao, Q., et al., 2011. Characteristics of PM2.5 speciation in representative megacities and across China. Atmos. Chem. Phys. 11 (11), 5207–5219.
Yao, L., Yang, L., Yuan, Q., et al., 2016. Sources apportionment of PM2.5 in a background site in the North China Plain. Sci. Total Environ. 541, 590–598.
Yin, J., Harrison, R.M., 2008. Pragmatic mass closure study for PM1.0, PM2.5 and PM10 at roadside, urban background and rural sites. Atmos. Environ. 42 (5), 980–988.
Yin, L., Niu, Z., Chen, X., et al., 2014. Characteristics of water-soluble inorganic ions in PM2.5 and PM2.5–10 in the coastal urban agglomeration along the Western Taiwan Strait Region, China. Environ. Sci. Pollut. Res. 21 (7), 5141–5156.
Zhang, Y.L., Cao, F., 2015. Fine particulate matter (PM2.5) in China at a city level. Sci. Rep. 5, 14884.
Zhang, X., Friedl, M.A., Schaaf, C.B., et al., 2004. The footprint of urban climates on vegetation phenology. Geophys. Res. Lett. 31 (12).
Zhang, R., Wang, G., Guo, S., et al., 2015. Formation of urban fine particulate matter. Chem. Rev. 115 (10), 3803–3855.
Zhang, H., Wang, S., Hao, J., et al., 2016. Air pollution and control action in Beijing. J. Clean. Prod. 112, 1519–1527.
Zhao, J., Chen, S., Jiang, B., et al., 2013. Temporal trend of green space coverage in China and its relationship with urbanization over the last two decades. Sci. Total Environ. 442, 455–465.
Zhou, L., Dickinson, R.E., Tian, Y., et al., 2004. Evidence for a significant urbanization effect on climate in China. PNAS 101 (26), 9540–9544.
Zhou, D., Zhao, S., Liu, S., et al., 2014a. Surface urban heat island in China's 32 major cities: spatial patterns and drivers. Remote Sens. Environ. 152 (152), 51–61.
Zhou, D., Zhao, S., Liu, S., et al., 2014b. Spatiotemporal trends of terrestrial vegetation activity along the urban development intensity gradient in China's 32 major cities. Sci. Total Environ. 488, 136–145.
Zhou, D., Zhao, S., Zhang, L., et al., 2015. The footprint of urban heat island effect in China. Sci. Rep. 5, 11160.
Zhou, J., Xing, Z., Deng, J., et al., 2016. Characterizing and sourcing ambient PM2.5 over key emission regions in China I: water-soluble ions and carbonaceous fractions. Atmos. Environ. 135, 20–30.
Zhou, D., Zhang, L., Hao, L., et al., 2016. Spatiotemporal trends of urban heat island effect along the urban development intensity gradient in China. Sci. Total Environ. 544, 617–626.
Zhu, Y.G., Ioannidis, J.P.A., Li, H., et al., 2011. Understanding and harnessing the health effects of rapid urbanization in China. Environ. Sci. Technol. 45, 5099–5104.